Three-Dimensional Viscous Flow Computations of High Area Ratio Nozzles for Hypersonic Propulsion

D. R. Reddy* and G. J. Harloff†
Sverdrup Technology Inc., NASA Lewis Research Center Group, Brook Park, Ohio 44142

The PARC3D code was selected by the authors to analyze a variety of complex and high-speed flow configurations. Geometries considered for code validation include ramps and corner flows, which are characteristic of inlets and nozzles. Flows with Mach numbers of 3–14 were studied. Both two- and three-dimensional experimental data for shock-boundary-layer interaction were considered to validate the code. A detailed comparison of various flow parameters with available experimental data is presented; agreement between the solutions and the experimental data in terms of pitot pressure profiles, yaw-angle distributions, static pressures, and skin friction is found to be very good. In addition, two- and three-dimensional flow calculations were performed for a hypersonic nozzle. Comparison of the wall pressure results with the published solutions is made for the two-dimensional case.

Nomenclature

ALFA	= yaw angle
Cp	= pressure coefficient, $=(P-PREF)/[OREF(UREF^2)]$
Cf	= skin-friction coefficient, =(wall shear)/$[OREF(UREF^2)]$
L	= length of leading-edge flat plate
P	= static pressure
PREF	= freestream static pressure
PS	= pitot pressure
PS(0)	= static pressure at nozzle entrance
PSREF	= freestream pitot pressure
OREF	= freestream density
UREF	= freestream velocity
X	= horizontal distance
XO	= entrance nozzle height
Xwall	= horizontal distance along the wall
Y	= normal distance
YG	= normal distance from shock generator surface
Z	= spanwise distance

Introduction

ACCURATE evaluation of nozzle performance is essential in hypersonic propulsion because the net thrust is very sensitive to nozzle performance. Highly integrated fuselage/nozzle configurations may experience complex interactions of shocks, turbulent mixing, differing levels of under- or over-expansion, and possible boundary-layer separation. A numerical method has been selected and used to examine the flow phenomena mentioned above. The model is calibrated herein using available experimental data in two and three dimensions.

The PARC3D[1] code, selected by the authors for this study, solves the full, three-dimensional, Reynolds-averaged, Navier-Stokes equations in strong conservation form with the Beam and Warming approximate factorization algorithm. The implicit scheme uses central differencing for a curvilinear set of coordinates. The code was originally developed as AIR3D by Pulliam and Steger[2]; Pulliam[3] later added the Jameson et al.[4] artificial dissipation and called the code ARC3D.

Cooper[1] adapted the ARC3D code for internal propulsion applications and named the code PARC3D. Cooper et al.[5] applied a two-dimensional version of PARC to a trumpet and a conical nozzle with a throat Reynolds number of 1.2×10^4. The ground-tested nozzles had expansion ratios of 362 and 400, and exhausted into low pressures of 3.8×10^{-7} to 6.2×10^{-3} psia. They concluded that the PARC code provided reasonable flowfields for the cases studied.

In order to gain confidence with the PARC3D code for high-speed applications, some shock-boundary-layer experimental data and published nozzle flowfield results were selected in the present study for code validation. Both two- and three-dimensional experimental data for shock-boundary-layer interaction were considered; a detailed comparison of various flow parameters is presented. In addition, two- and three-dimensional flow calculations were performed for a hypersonic nozzle. Comparison of the wall pressure results with the published solutions was made for the two-dimensional case; the solutions agree very well with the experimental data for the shock-boundary-layer interaction cases and with other numerical solutions for the hypersonic nozzle configuration.

Previous Studies

Shock-Boundary-Layer Interaction

Many researchers have studied two- and three-dimensional shock-boundary-layer interactions in the past. For example, Visbal[6] evaluated the Baldwin-Lomax[7] turbulence model for a two-dimensional Mach 3 compression corner with a Reynolds-averaged Navier-Stokes computer program. He ex-

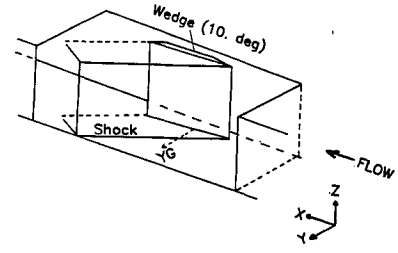

Fig. 1 Experimental configuration for three-dimensional shock-boundary-layer interaction.

Presented as Paper 88-0474 at the AIAA 26th Aerospace Sciences Meeting, Reno, NV, Jan. 11–14, 1988; received July 15, 1988; revision received July 13, 1989.

*Supervisor, Turbomachinery Analysis Section. Member AIAA.
†Senior Staff Scientist. Associate Fellow AIAA.

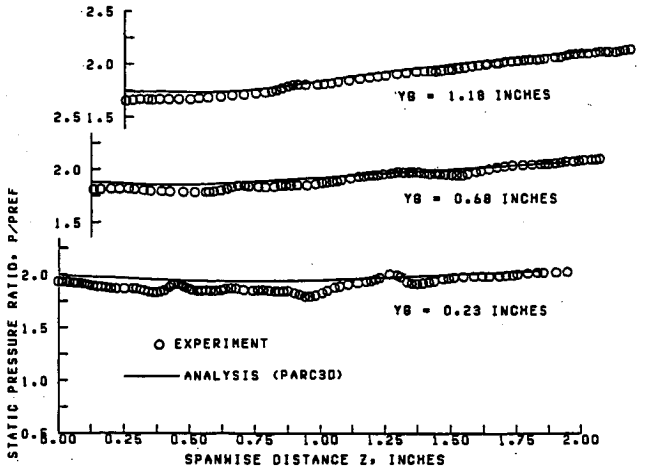

Fig. 2a Static pressure surveys for coarse grid; $X = 5.10$ in.

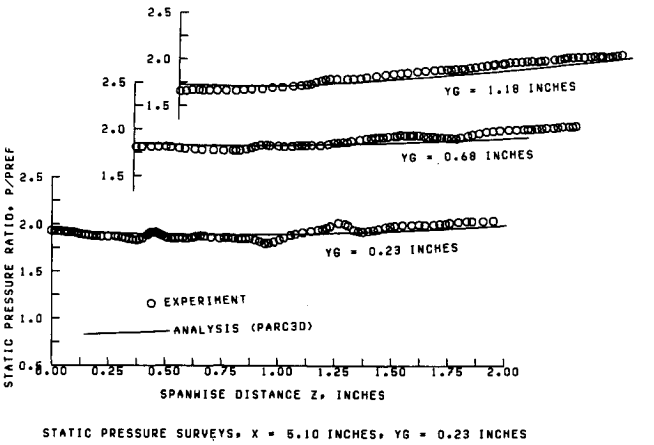

Fig. 2b Static pressure surveys for fine grid; $X = 5.10$ in.

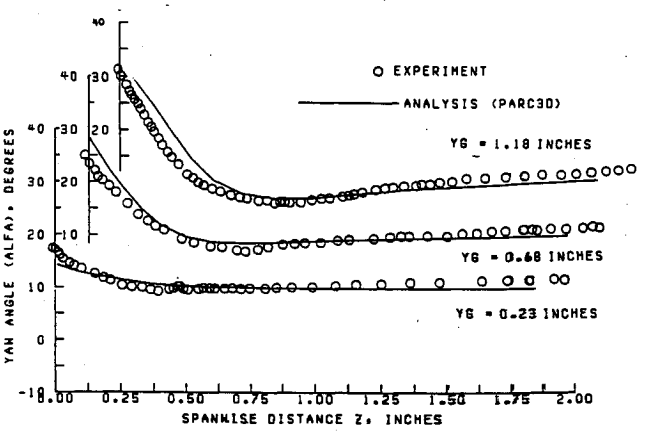

Fig. 3a Yaw-angle surveys for coarse grid; $X = 5.10$ in.

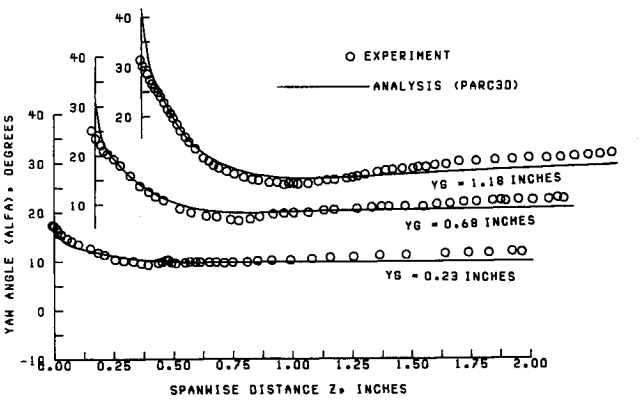

Fig. 3b Yaw-angle surveys for fine grid; $X = 5.10$ in.

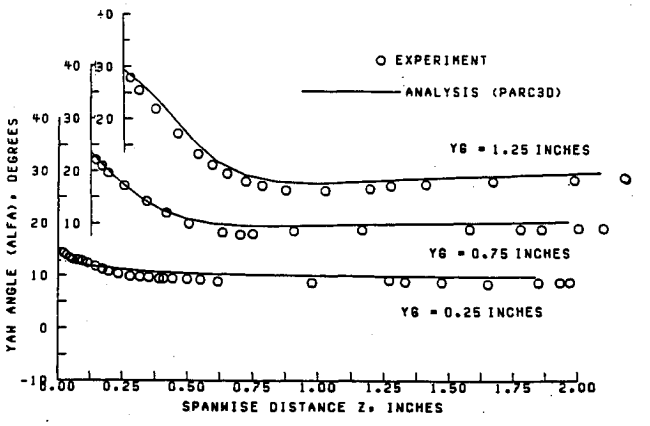

Fig. 4a Yaw-angle surveys for coarse grid; $X = 7.10$ in.

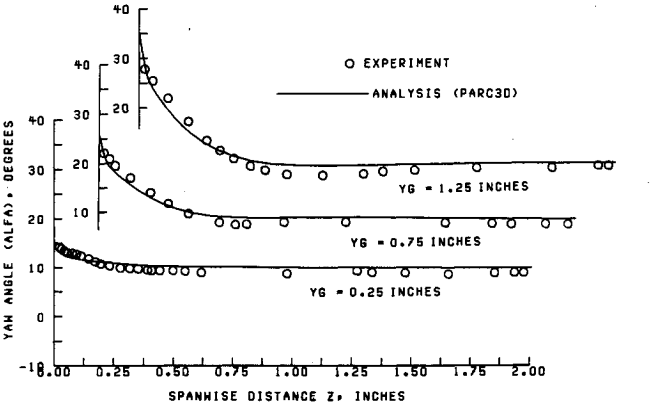

Fig. 4b Yaw-angle surveys for fine grid; $X = 7.10$ in.

amined attached and separated flows and concluded that some of the constants in the outer formulation of the Baldwin-Lomax model are dependent on the flow Mach number. Horstman[8] presented experimental and theoretical three-dimensional solutions for a family of fin-induced, shock-wave turbulent boundary-layer interactions with separated flow at Mach number 2.94 with fin angles from 10 to 20 deg; he used the MacCormack explicit second-order predictor-corrector finite-volume method. Knight[9,10] used a hybrid explicit-implicit method to solve the three-dimensional sharp fin interaction at Mach 3 with a wedge angle of 10 deg. Lawrence et al.[11] presented an upwind scheme for parabolized Navier-Stokes equations and calculated the flowfields for a 15-deg compression corner and a hypersonic inlet.

Anderson and Benson[12] studied three-dimensional shock-boundary-layer interactions in calibrating a single sweep space marching code, PEPSIS. They showed good comparisons for the Oskam et al.[13] three-dimensional shock-boundary-layer configuration.

Holden and Moselle[14] studied experimentally several two-dimensional ramp configurations in hypersonic flow. Hung and MacCormack[15] as well as Lawrence and Tannehill[11] have previously computed the flowfield for a few of Holden and Moselle's[14] ramp configurations.

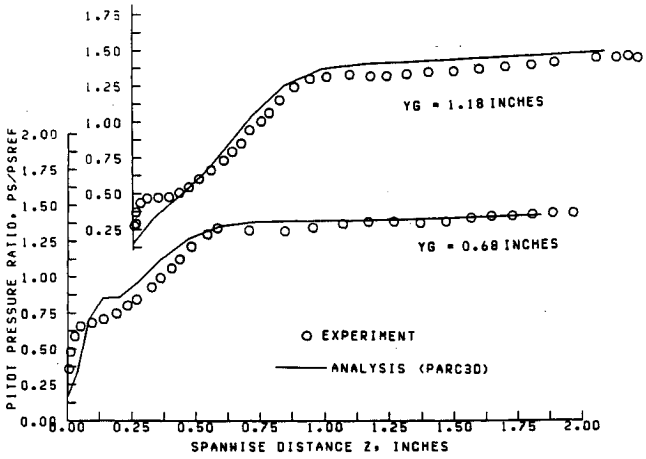

Fig. 5a Pitot pressure surveys for coarse grid; $X = 5.1$ in.

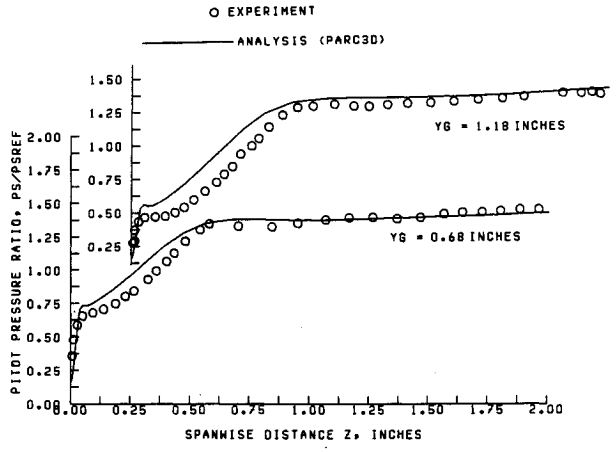

Fig. 5b Pitot pressure surveys for fine grid; $X = 5.1$ in.

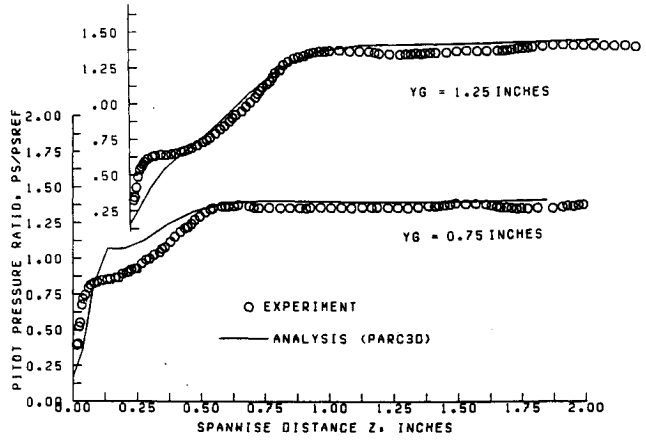

Fig. 6a Pitot pressure surveys for coarse grid; $X = 7.1$ in.

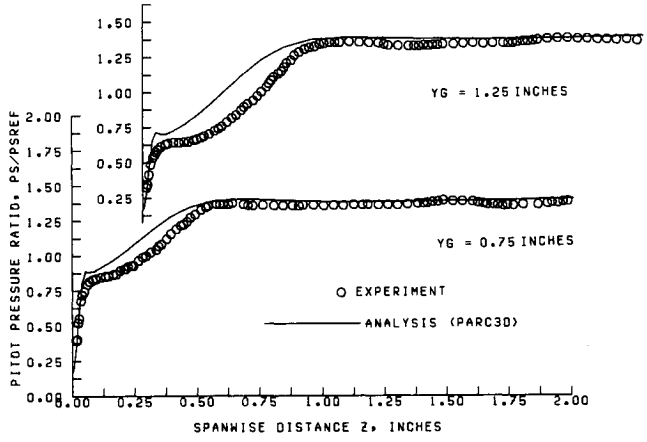

Fig. 6b Pitot pressure surveys for fine grid; $X = 7.1$ in.

Nozzles

Dash et al.[16] presented a parabolized Navier-Stokes nozzle capability in two and three dimensions to calculate mixed supersonic and subsonic flows. Pressure-split and sublayer approximations were used to obtain solutions by spatial marching. A method-of-characteristics study by Lewis et al.[17] examined a cutoff nozzle to investigate the effect of internal to external expansion on thrust-vectored lift of asymmetric nozzles with a truncated lower cowl.

Code Validation

In order to assess the capability of the PARC3D code in simulating the interaction phenomenon characteristic of hypersonic nozzle flow, some shock-boundary-layer experimental data and a published nozzle flowfield study were selected for comparison. Both two- and three-dimensional shock-boundary-layer interaction experimental data were considered. Two sets of data were examined: the three-dimensional flowfields of Oskam et al.[13] at Mach 2.94, and the two-dimensional flow of Holden and Moselle[14] at Mach 14.1.

Results and Discussion

Three-Dimensional Shock-Boundary-Layer Calculations at Mach 2.94

Figure 1 shows the schematic of the experimental three-dimensional configuration from Ref. 13. The details of the experimental rake locations can be found in Refs. 12 and 13. The data measured include yaw angle as well as static and pitot pressure profiles. In the experimental setup, the wedge was mounted off the wall to avoid the wall boundary layer at the leading edge of the wedge; however, the boundary layer

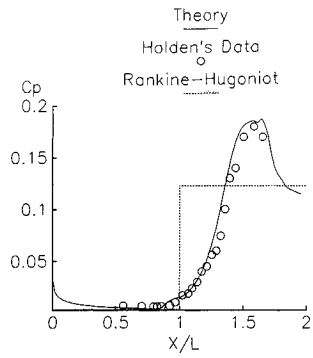

Fig. 7 *Cp* on 18-deg ramp at Mach = 14.1.

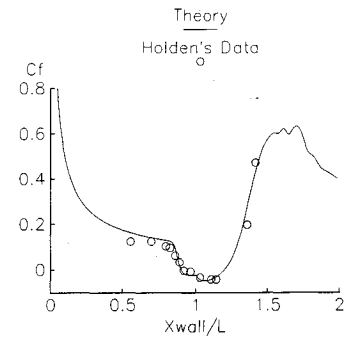

Fig. 8 *Cf* on 18-deg ramp at Mach = 14.1.

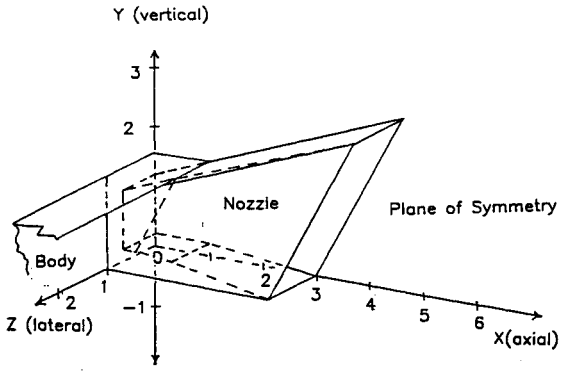

Fig. 9 Schematic of three-dimensional nozzle.

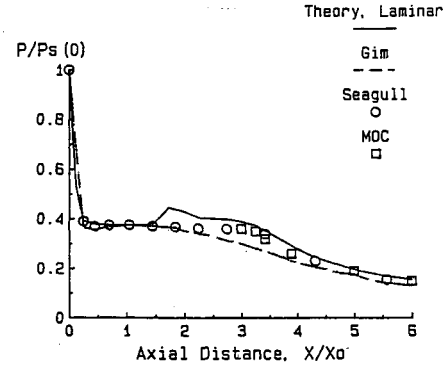

Fig. 10 Upper-wall static pressure vs distance; two-dimensional nozzle calculations.

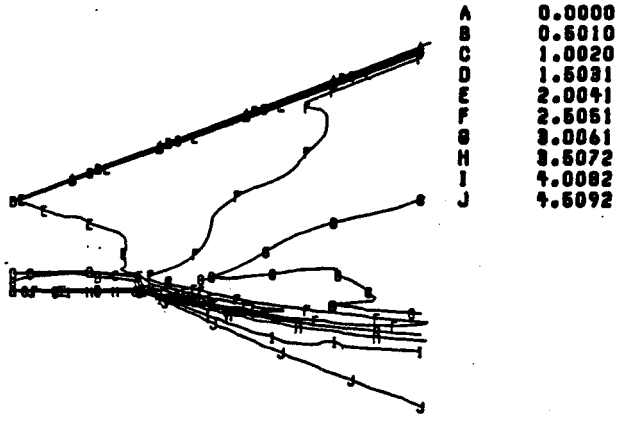

Fig. 11 Mach numbers for two-dimensional nozzle.

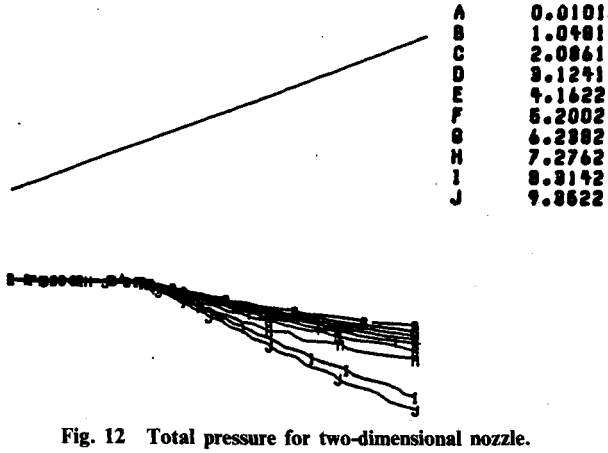

Fig. 12 Total pressure for two-dimensional nozzle.

on the side wall ($Z = 0$) was undisturbed in the entry plane. The wedge angle was 10 deg as shown in Fig. 1. The freestream Mach number was 2.94, and the Reynolds number, based on wind-tunnel test section height (8 in. or 20.32 cm) and total conditions, was 58.9×10^6.

The computational grid used in this study was $121 \times 81 \times 41$. To assess grid-resolution effects on the solution, a finer mesh of $121 \times 101 \times 61$ was also used. Symmetry was assumed in the transverse Z direction in the computations. In these computations, a small flow angularity in the Y direction, up to a maximum of 1 deg, was specified to account for the normal velocity resulting from boundary-layer growth upstream of the wedge.

Plots of static-pressure rake surveys are shown in Fig. 2a for the coarse-grid case, for the rake location of 5.1 in. (12.95 cm), and for different distances from the wedge YG (see Fig. 1). Reasonable agreement of the solutions with the experimental data can be seen from the comparison. The corresponding fine-grid solution is shown in Fig. 2b. As expected, the agreement between the solution and the data improves with the finer grid, especially near the wall. Yaw-angle distributions for rake locations of 5.1 and 7.1 in. (12.95 and 18.03 cm) are shown in Figs. 3a and 4a for the coarse grid. Good agreement is also evident for the yaw angles. In the near wall region, the finer-grid results show much better agreement as shown in Figs. 3b and 4b, respectively. Note that

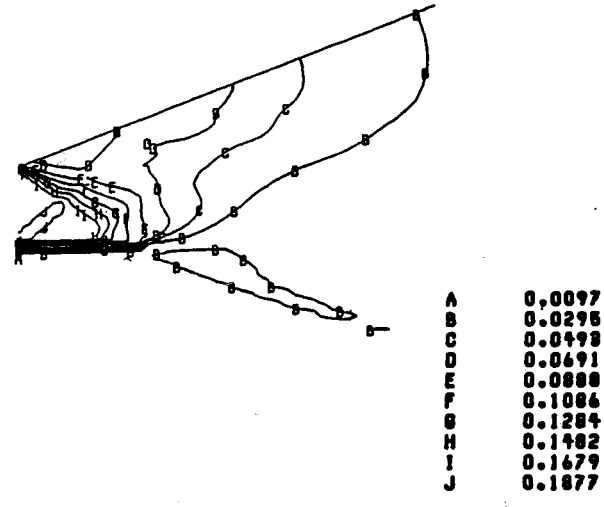

Fig. 13 Static pressure for two-dimensional nozzle.

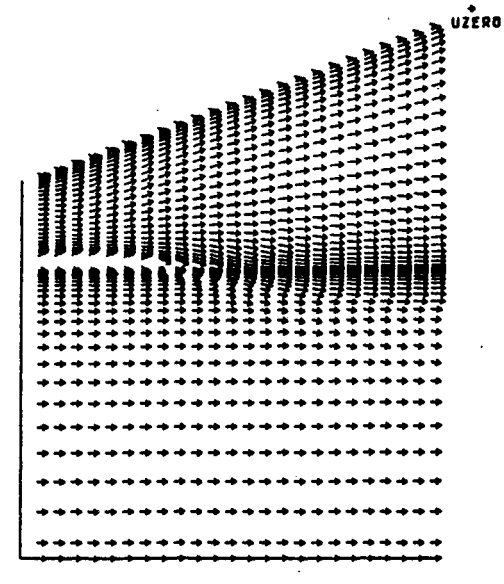

Fig. 14 Velocity vectors for two-dimensional nozzle.

the 20-deg variation of yaw angles through the side wall boundary layer is well predicted by the theory. Pitot pressures, presented as the ratio of local pitot pressure to the freestream pitot pressure, through the boundary layer at rake locations of 5.1 and 7.1 in. (12.95 and 18.03 cm) are presented for the coarse-grid case in Figs. 5a and 6a; the computed and experimental pitot pressure values agree well in the outer portion of the boundary layer, farther than 0.25 in. (0.63 cm) from the wall. The fine-grid results presented in Figs. 5b and 6b show much better agreement near the wall than the coarse-grid results. Additional grid refinement in the shock-boundary-layer interaction region away from the wall should further improve the comparison. Studies involving different amounts of artificial viscosity were performed with little effect on the results.

Two-Dimensional Shock-Boundary-Layer Interaction at Mach 14.1

The two-dimensional experimental data of Holden and Moselle[14] at Mach 14.1 were used as a hypersonic test case. The leading-edge flat plate was 1.44 ft (43.89 cm) long, the ramp angle 18 deg, and the ramp length 1.14 ft (34.75 cm). The Reynolds number per foot based on total conditions was 22.2×10^6. The computational grid used in the present study was 399×99.

The predicted surface-pressure coefficient is shown in Fig. 7 compared to the test data; good agreement is evident from the comparison. The flow was assumed to be laminar in these calculations. The skin-friction distribution along the ramp surface is shown in Fig. 8; the agreement with experimental data is very good. Note that a small region of reversed flow, just upstream of the ramp corner, can be seen from the negative skin-friction values in Fig. 8.

Nozzle Flowfield Calculations

Geometry

The three-dimensional nozzle is shown schematically in Fig. 9 (from Spradley et al.[18]). The nozzle length is six entrance nozzle heights, and the upper wall is linear with a 20-deg slope. The lower splitter length is three entrance nozzle heights. The lower wall is horizontal up to one nozzle height where the wall expands at a 6-deg angle (see Fig. 9). The two-dimensional geometry expressions were taken from Ref. 19, and the three-dimensional geometry considered for the computations was taken from Ref. 18. Note that the aft portion of the nozzle differs from that of Ref. 19.

Two-Dimensional Flowfield Calculations

Two-dimensional nozzle flowfield calculations are presented for the nozzle analyzed by Spradley et al.[18] The same region of flow that was analyzed by Spradley et al. is analyzed here, i.e., to six nozzle entrance heights in the flow direction. The grid used in the present computation was 199×99.

The nozzle entrance flow was assumed to be uniform. The ratio of specific heats was 1.27 for both streams. The nozzle entrance velocity was 1610 m/s, the static pressure 9206.3 Pa, the static temperature 2311 K, and the Mach number 1.657. The corresponding freestream values were 1765 m/s, 506.2 Pa, 261 K, and 5.0, respectively.[18] The upper-wall static pressures, nondimensionalized by the nozzle entrance total pressue, are shown in Fig. 10. Also shown in the figure are values from the GIM[18] code, the SEAGULL[20] code, and a method-of-characteristics code (MOC).[18] The pressures near the nozzle entrance are in agreement with the GIM results and are higher in the aft region. The inviscid results of SEAGULL and MOC lie between the current viscous solution and the GIM solution in this region.

The predicted flowfield is presented in terms of Mach number, static pressure, total pressures contours, and velocity vectors in Figs. 11–14, respectively. The static and total pressures presented in these and the subsequent figures are normalized by the nozzle entrance total pressure and the ratio

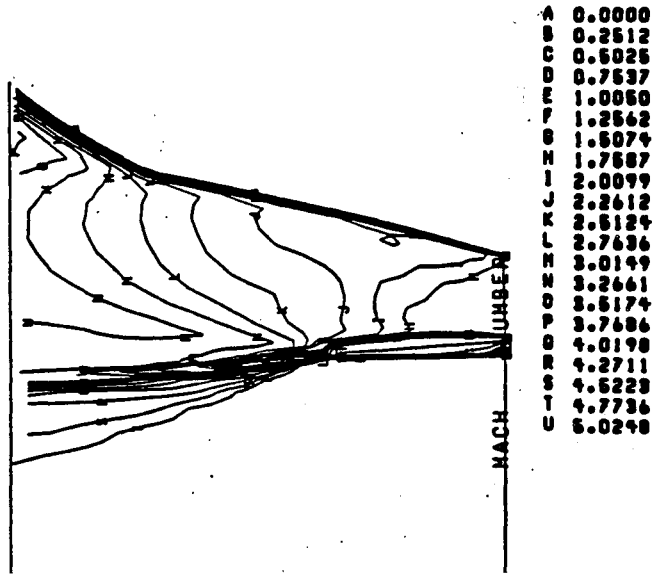

Fig. 15 Mach numbers at $Z = 0.473$.

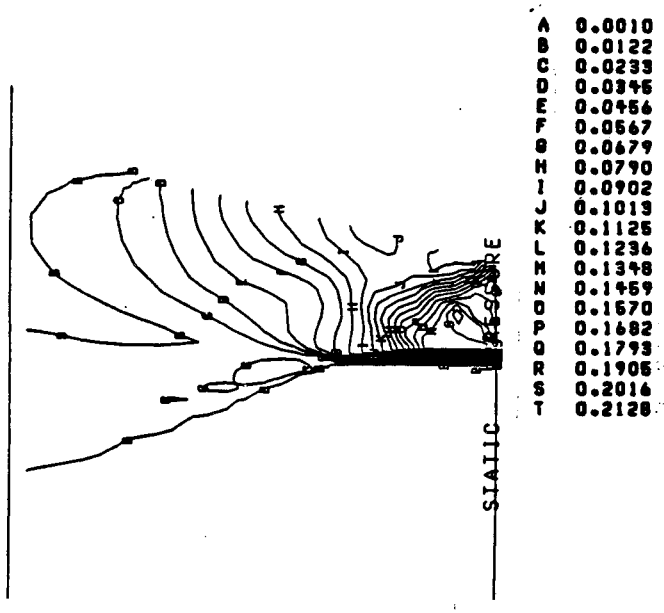

Fig. 16 Static pressure at $Z = 0.473$.

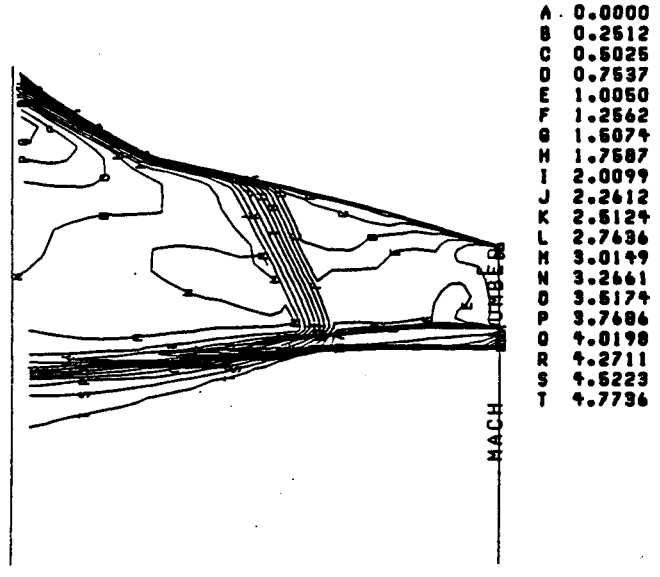

Fig. 17 Mach numbers at $Z = 1.06$.

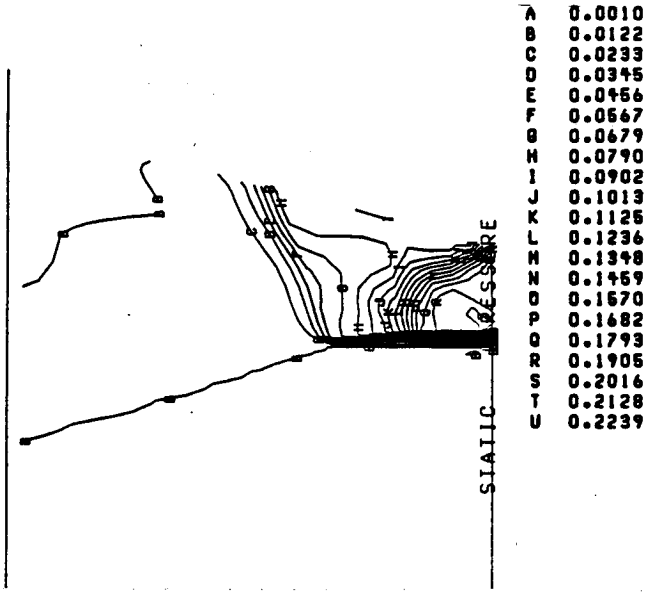

Fig. 18 Static pressure at $Z = 1.06$.

of specific heats. The contact surface between the nozzle flow and the freestream is evident in the total pressure contour plot. The corresponding variation in the Mach lines is shown in the Mach-number contours. Note that the jet is deflected downward, as shown in the velocity vectors, indicating that the nozzle flow is underexpanded.

Three-Dimensional Nozzle Flowfield Calculations

The three-dimensional geometry is similar to the two-dimensional geometry in that the lower cowl has a 6-deg expansion and a 20-deg upper wall. The outer nozzle wall expands by 6 deg.

The following boundary conditions were used:

1) No slip on all walls; adiabatic wall temperature (no slip was specified all along the top surface).

2) Freestream boundary at $Z = 6$ (outer boundary in Z direction).

3) Freestream boundary at $Y = -3$ (lower boundary in Y direction).

4) Extrapolated conditions at the exit.

5) Symmetry at $Z = 0$ (inner boundary in Z direction).

The same nozzle entrance and freestream conditions as those of the two-dimensional configuration are used here. The computational grid used for this configuration was $111 \times 61 \times 51$.

The flowfield is presented in terms of Mach and static pressure contours in Figs. 15–18, at planes $Z = 0.473$ and 1.06 nozzle heights, respectively. The nozzle width is one nozzle height. The 0.473 plane is close to the nozzle center and the 1.06 plane is just outside the nozzle. The center plane flowfield is similar to the two-dimensional flowfield presented in Figs. 11 and 12. The 1.06 plane shows the effect of the side relief on the flowfield.

Summary

The PARC3D code has been validated for a variety of complex and high-speed flow configurations. The results were compared with experimental data where possible with very good agreement and reveal that the code can handle a wide variety of geometries, including ramps and corner flows characteristic of inlets and nozzles. Flows with Mach numbers of 3–14 were studied; phenomena of shock-boundary-layer interaction and shear-layer mixing were considered. Thus, this study demonstrates the capability of the PARC code to analyze three-dimensional viscous flows through high-speed propulsion components of practical interest.

Acknowledgments

Prepared for the NASA Lewis Research Center under Contracts NAS 3-24105 and NAS 3-25266, project managers B. Anderson and T. Benson. T. Benson's assistance in providing the digitized data for the Oskam et al.[13] configuration and support with the plotting software is appreciated. A major portion of the computational results was obtained using the Numerical Aerodynamic Simulation (NAS) computation facility located at NASA Ames Research Center, Moffett Field, California.

References

[1]Cooper, G. K., "The Parc Codes," Arnold Engineering Development Center, Tullahoma, TN, AEDC-TR-87-24, Oct. 1987.

[2]Pulliam, T. H., and Steger, J. L., "Implicit Finite-Difference Simulations of Three-Dimensional Compressible Flow," *AIAA Journal*, Vol. 18, No. 2, 1980, pp. 159–167.

[3]Pulliam, T. H., "Euler and Thin Layer Navier-Stokes Codes: ARC2D, ARC3D," Notes for Computational Fluid Dynamics User's Workshops, Univ. of Tennessee Space Inst., Tullahoma, TN, UTSI Pub. E02-4005-023-84, 1984, pp. 15.1–15.85.

[4]Jameson, A., Schmidt, W., and Turkel, E., "Numerical Solutions of the Euler Equations by Finite-Volume Methods Using Runge-Kutta Time-Stepping Schemes," AIAA Paper 81-1259, June 1981.

[5]Cooper, G. K., Jordan, J. L., and Phares, W. J., "Analysis Tool for Application to Ground Testing of Highly Underexpanded Nozzles," AIAA Paper 87-2015, June–July 1987.

[6]Visbal, M., "Numerical Simulation of Shock/Turbulent Boundary-Layer Interactions over 2-D Compression Corners," Ph.D. Dissertation, Rutgers Univ., New Brunswick, NJ, Oct. 1983.

[7]Baldwin, B., and Lomax, H., "Thin-Layer Approximation and Algebraic Model for Separated Flows," AIAA Paper 78-257, Jan. 1978.

[8]Horstman, C. C., "Computation of Sharp-Fin Induced Shock Wave/Turbulent Boundary-Layer Interactions," AIAA Paper 86-1032, May 1986.

[9]Knight, D. D., "Numerical Simulation of Three-Dimensional Shock-Turbulent Boundary-Layer Interaction Generated by a Sharp Fin," AIAA Paper 84-1559, June 1984.

[10]Knight, D. D., "A Hybrid Explicit-Implicit Numerical Algorithm for the Three-Dimensional Compressible Navier-Stokes Equations," AIAA Paper 83-0223, Jan. 1983.

[11]Lawrence, S. L., Tannehill, J. C., and Chaussee, D. S., "An Upwind Algorithm for the Parabolized Navier-Stokes Equations," AIAA Paper 86-1117, May 1986.

[12]Anderson, B. H., and Benson, T. J., "Numerical Solution to the Glancing Sidewall Oblique Shock-Wave/Turbulent-Layer Interaction in Three Dimensions," AIAA Paper 83-0136, Jan. 1983.

[13]Oskam, B., Vas, I. E., and Bogdonoff, S. M., "Oblique Shock Wave/Turbulent Boundary-Layer Interactions in Three Dimensions at Mach 3, Pt. I," Air Force Flight Dynamics, Wright-Patterson Air Force Base, OH, AFFDL-TR-76-48, June 1976.

[14]Holden, M. S., and Moselle, J. R., "Theoretical and Experimental Studies of the Shock-Wave-Boundary-Layer Interaction on Compression Surfaces in Hypersonic Flow," Aerospace Research Lab., Office of Aerospace Research, Wright-Patterson Air Force Base, OH, CAL Rept. AF-2410-A-1, Oct. 1969.

[15]Hung, C. M., and MacCormack, R. W., "Numerical Solutions of Supersonic and Hypersonic Laminar Flows over a Two-Dimensional Compression Corner," AIAA Paper 75-2, Jan. 1975.

[16]Dash, S. M., Wolf, D. E., Sinha, N., and Lee, S. H., "Progress in the Development of Parabolized Navier-Stokes (PNS) Methodology for Analyzing Propulsive Jet Mixing Problems," AIAA Paper 86-1115, May 1986.

[17]Lewis, W. G. E., Herd, R. J., and Herbert, M. V., "Lift Characteristics of Asymmetric Exhaust Nozzles at High Flight Speeds," *Journal of the Royal Aeronautical Society*, Vol. 70, Nov. 1966, pp. 1036–1040.

[18]Spradley, L. W., Anderson, P. G., and Pearson, M. L., "Computations of Three-Dimensional Nozzle-Exhaust Flowfields with the GIM Code," NASA CR-3042, Aug. 1978.

[19]Oman, R. A., Forman, K. M., Leng, J., and Hopkins, H. B., "Simulation of Hypersonic Scramjet Exhaust," NASA CR-2494, March 1975.

[20]Salas, M. D., "Shock-Fitting Method for Complicated Two-Dimensional Supersonic Flows," *AIAA Journal*, Vol. 4, No. 5, 1976, pp. 583–588.